

Analysis of a Co-Flow Mixer in Preparation of Combustor-Turbine Matching in a Rotating Detonation Engine

Uhl, G.^{1,2,3}, Odier, N.³, Dombard, J.³, Zurbach, S.¹, Poinso, T.³, Bellenoue, M.²

✉ gregory.uhl@safrangroup.com

¹Safran Tech, E&PC, Rue des Jeunes Bois - Châteaufort, 78114 Magny-Les-Hameaux, France

²ISAE-ENSMA, Institute PPRIME, Department FTC, 1 Avenue Clément Ader, 86961 Chasseneuil-du-Poitou, France

³CERFACS, 42 Avenue Gaspard Coriolis, 31100 Toulouse, France

1. Introduction

- Climate change and consequent emission constraints, paired with an expected increase in air passengers [1] and global energy demand [2] in the next decades, require the development and operation of high-efficiency, low-emission turbomachines in both the energy and aviation sectors. However, over the last decades, gas turbine technology has advanced to a very mature level by optimizing component performance, and it is expected that further improvement would only marginally increase the overall gas turbine efficiency [3].
- To this end, Pressure Gain Combustion (PGC) devices that incorporate an alternative thermodynamic cycle have been under investigation. A notable example is the Rotating Detonation Combustor (RDC), where one or several detonation waves are circulating around a typically annular combustion chamber. A particular characteristic of RDCs is their high-frequency, high-temperature, high-speed exhaust flow that may have a detrimental effect on combustor-turbine coupling in a turbomachinery application [4].
- In an effort to temper this phenomenon, a co-flow mixer is investigated using 1D analytical modeling and a Large-Eddy Simulation (LES). The component entrains subsonic secondary air, aiming at an energy transfer from exhaust to entrained flow.
- Although not abundant in literature, some studies have shown the feasibility of the concept [4,5].

2. Project Overview

Geometry

- A 2D layout of the annular component is presented in fig. 1. The design relied on a previous study [5], and was adapted to the TU Berlin RDC test rig [3].

Cycle integration

- The component is placed between combustor outlet and subsonic turbine inlet, as evident from fig. 2. The entrained, secondary air bypasses the combustion chamber before entering the mixer.

Design requirements

- Without any attenuation of the exhaust gas, the pressure gain inherent to RDCs may diminish in the subsonic turbine due to an inefficient operating condition [4]. Hence, at the mixer outlet, a reduction in both peak values and fluctuations in temperature and flow velocity is required, along with a reduction in pressure fluctuations.
- However, this attenuation is constrained by the total pressure loss, which should be minimal along the mixer axis.

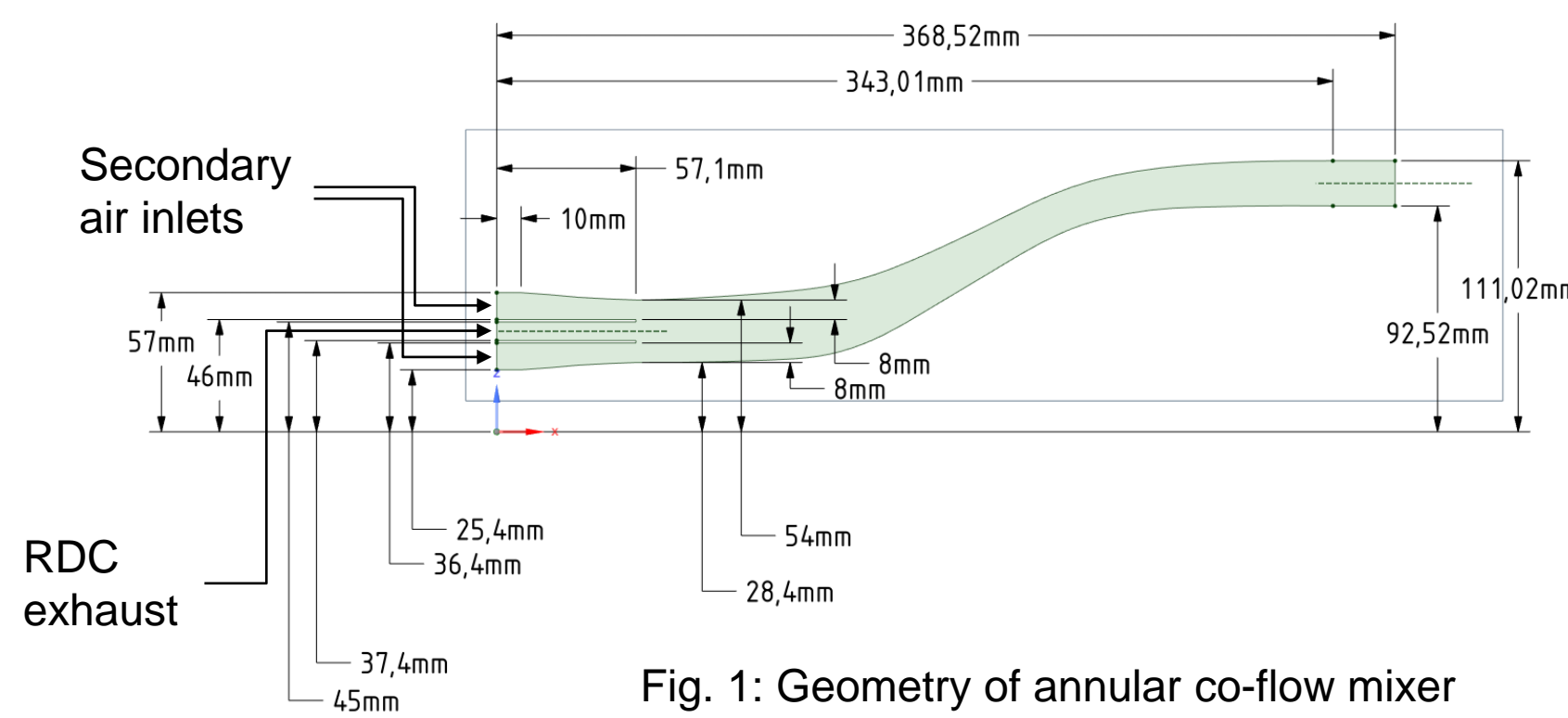


Fig. 1: Geometry of annular co-flow mixer

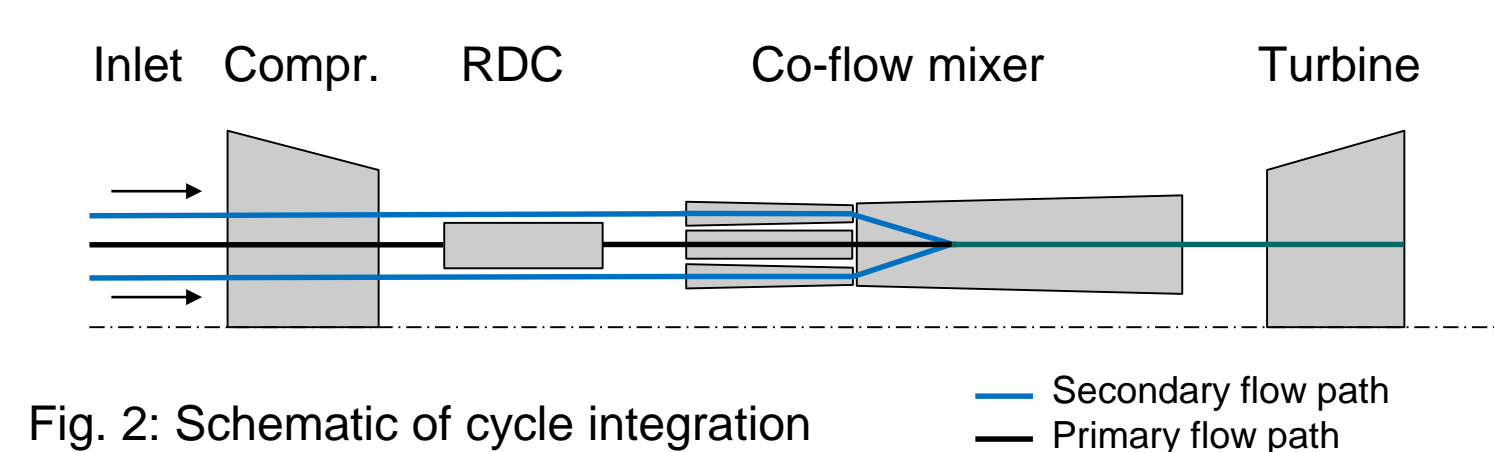


Fig. 2: Schematic of cycle integration

3. 1D Modeling

- The 1D model under development for the co-flow mixer relies on the generalized compressible flow approach, as documented by Shapiro [6]. In order to apply the theory, a transformation of the original geometry (fig. 1) into 1D was necessary, depicted in fig. 3 with the imposed boundary conditions.

- The following assumptions were adopted:

- 1D, steady, adiabatic flow
- No work extraction
- Both flows are ideal gases with piecewise c_p, γ, W
- Mixing takes place between station 143 and *conf*

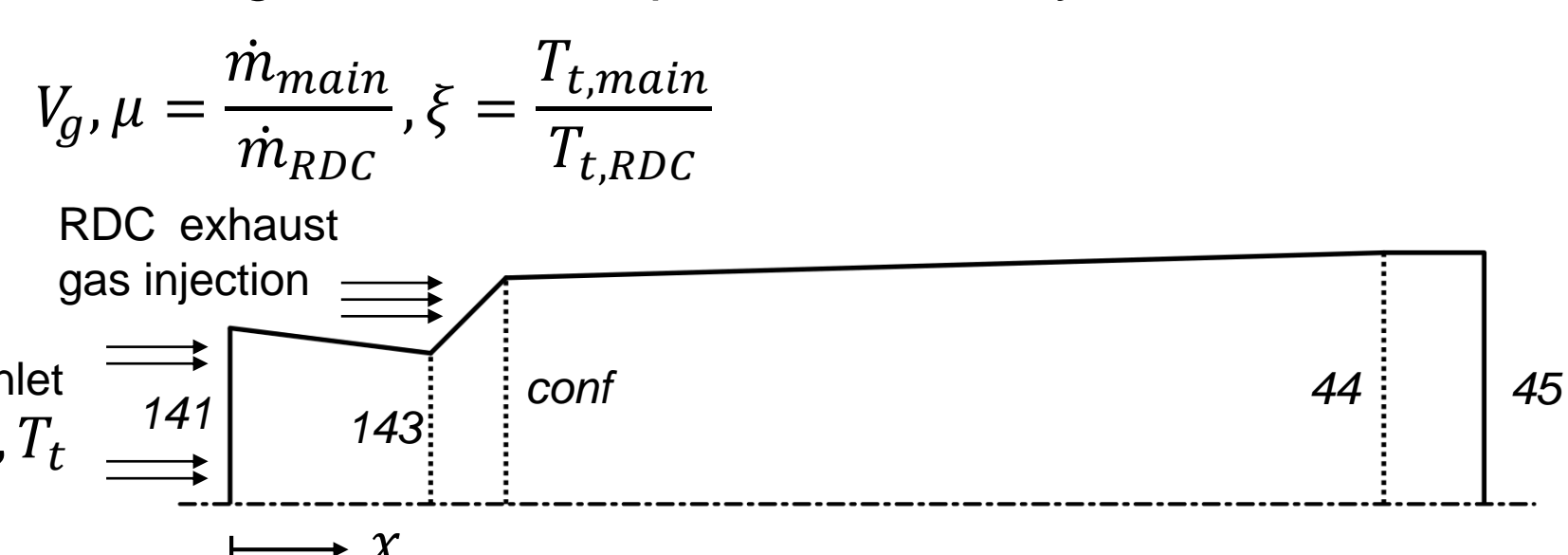


Fig. 3: 1D model of co-flow mixer, with axial stations indicated

- Governing equation [6]:

$$\frac{dM^2}{M^2} = - \underbrace{\frac{2\psi}{1-M^2} \frac{dA}{A}}_{\text{area}} + \underbrace{\frac{1+\gamma M^2}{1-M^2} \frac{dH}{c_p T}}_{\text{enthalpy}} + \underbrace{\frac{\gamma M^2 \psi}{1-M^2} \left[4f \frac{dx}{D} - 2 \frac{V_g d\dot{m}}{V \dot{m}} \right]}_{\text{momentum (friction, mass injection)}} + \underbrace{\frac{2(1+\gamma M^2)\psi}{1-M^2} \frac{d\dot{m}}{\dot{m}}}_{\text{mass flow}} - \underbrace{\frac{1+\gamma M^2}{1-M^2} \frac{dW}{W}}_{\text{molecular weight}} - \underbrace{\frac{d\gamma}{\gamma}}_{\text{heat capacities}}$$

with $\psi = 1 + \frac{\gamma-1}{2} M^2$, friction factor f , hydraulic diameter D and streamwise injected gas velocity V_g .

- The secondary flow is modeled as the main flow, and the RDC exhaust gas as the "injected" flow, since the bypass mass flow rate is expected to be higher than the RDC exhaust [5].
- Solving the equation requires modeling the highlighted driving potentials as functions over the axial coordinate. In a first approximation, linear functions were adopted. Moreover, an axial discretization of the mixer was necessary for the numerical integration.
- The unsteadiness of the exhaust gas will be taken into account by a quasi-stationary approach.
- In its current version, the model does not support a sonic point transition (singularity at $M = 1$), nor is normal shock imposition considered. Both will be implemented in future versions.

4. Numerical Setup for LES

- The numerical simulations were done using AVBP, a compressible, multi-species code solving the filtered Navier-Stokes equations for LES [7]. Towards a further verification of the 1D analytical model, the numerical campaign was initiated with a 2D computation. In addition, utilizing results from both 1D and 2D modeling, a corresponding 3D case for an annular section was performed.

2D Computation

- The 2D computation was done on an unstructured, fully triangular mesh, with 88612 elements.
- Stationary boundary conditions were employed, summarized in tab. 1. The inlet data were approximated from literature ([3], [5]), whereas the outlet static pressure was inferred from the 1D model.
- All walls were modeled using a law-of-the-wall.

Secondary flow inlet	Air	$P_t = 0.5 \text{ MPa}$ $T_t = 600 \text{ K}$
RDC exhaust gas inlet	Mixture with $Y_{N_2} = 0.745, Y_{H_2O} = 0.255$	$V = 750 \text{ m/s}$ $T_s = 2238 \text{ K}$
Outlet		$P_s = 0.45 \text{ MPa}$

Tab. 1: Boundary conditions imposed in 2D computation

3D Computation

- The 3D computation was performed on a fully tetrahedral mesh for an annular section of 24 deg with 13.6 million elements, see fig. 4. The minimum element volume was $0.2e-13 \text{ m}^3$.
- The imposed boundary conditions were inferred from the 2D computation, with periodicity for the side boundaries.



Fig. 4: Fully tetrahedral mesh employed for the 3D case.

4. Results and Discussion

- Results comparing the predictions from 1D model and 2D computation are presented in fig. 5. Evidently, there are considerable differences, especially in the mixing zone. It should be noted that in the 1D model, the mixing process is idealized and terminates quickly, as described in section 3.
- However, for the selected operating point, the 1D model seems to roughly reproduce the boundary values calculated with AVBP. The total pressure loss is underestimated by the 1D model.

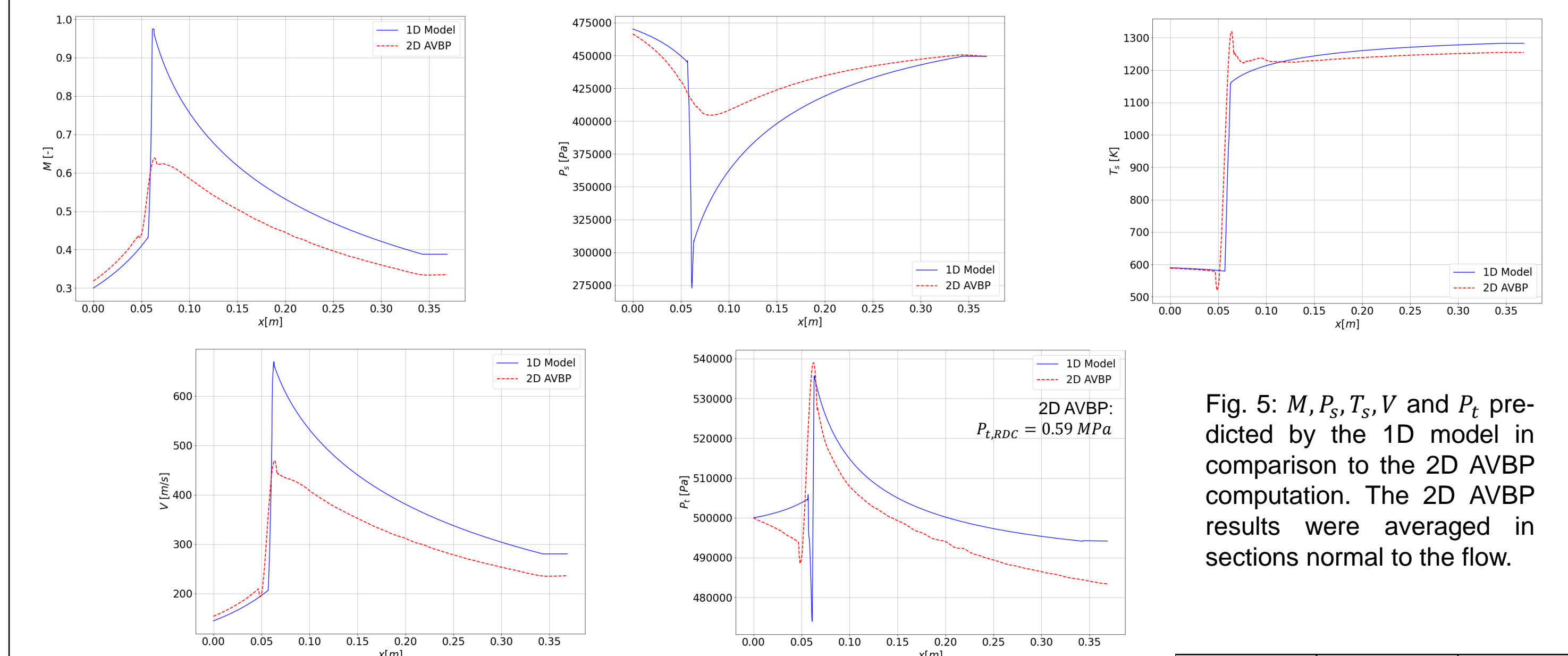


Fig. 5: M, P_t, T_s, V and P_t predicted by the 1D model in comparison to the 2D AVBP computation. The 2D AVBP results were averaged in sections normal to the flow.

- In tab. 2, the entrainment ratio and the total temperature ratio are compared. Both values are in the same order of magnitude than imposed by the 1D model.
- The total pressure loss (with respect to the RDC inlet) calculated with 2D AVBP can be quantified as:

$$\delta_{2D} = \frac{P_{t,outlet} - P_{t,RDC}}{P_{t,RDC}} = -0.18$$

	1D Model	2D AVBP
$\mu = \frac{\dot{m}_{main}}{\dot{m}_{RDC}}$	1.7	2.0
$\xi = \frac{T_{t,main}}{T_{t,RDC}}$	0.25	0.25

Tab. 2: Entrainment ratio and total temperature ratio for the 1D model, compared to the 2D AVBP calculation.

- In fig. 6, the total pressure, static temperature and flow velocity (x -direction) are presented for the 3D case. The results confirm the ability of the mixer to decelerate and cool the RDC exhaust gas, at a loss in total pressure.
- As predicted by the 1D model, there is an absence of normal shocks along the mixer length. Moreover, the magnitude of the presented 3D results matches the 1D and 2D predictions.
- The shock train exiting the primary flow channel is dissipated by the entrained secondary air.

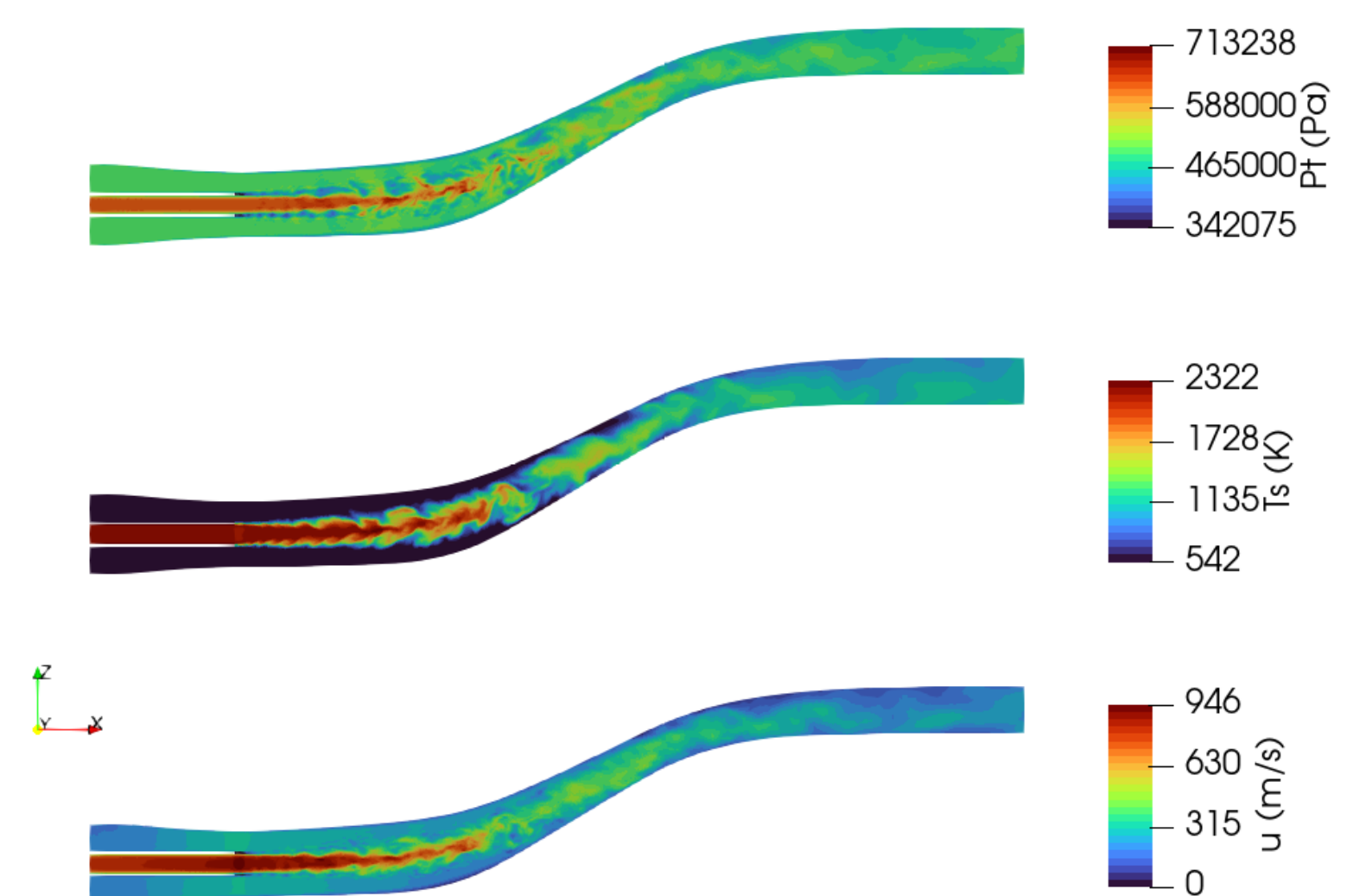


Fig. 6: P_t, T_s and V for the 3D case after a physical time of 0.01s.

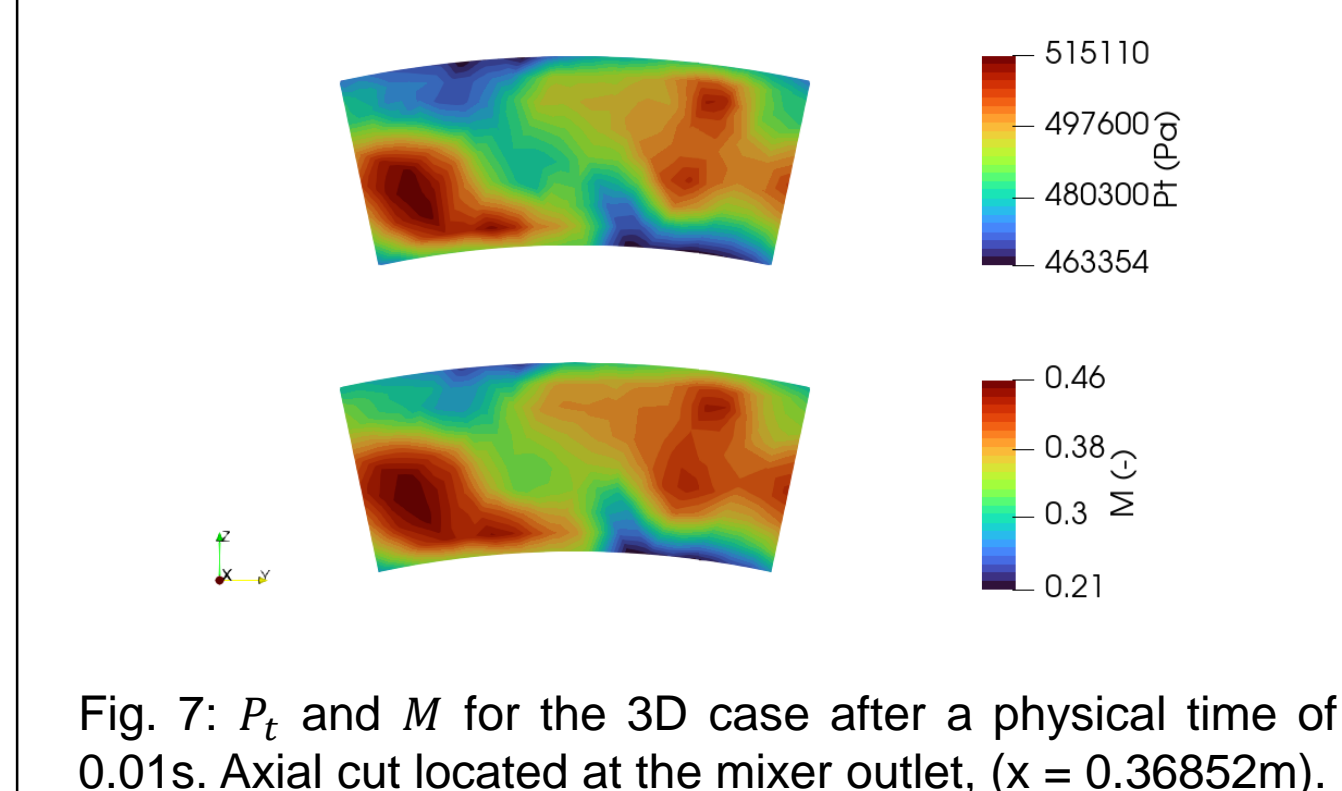


Fig. 7: P_t and M for the 3D case after a physical time of 0.01s. Axial cut located at the mixer outlet, ($x = 0.36852\text{m}$).

- The outlet plane colored with Mach number and total pressure is presented in fig. 7. For both quantities, a spatially varying field can be observed.
- The loss in total pressure in the 3D computation was obtained by averaging P_t on all computed nodes in the RDC inlet and domain outlet patches, respectively, and amounted to $\delta_{3D} = -0.23$.

5. Conclusions and Outlook

- The preliminary results for the operating point investigated underlined the ability of the co-flow mixer to reduce flow velocity and static temperature along its length, although at a non-negligible loss in total pressure compared to the experimentally obtained pressure gain in RDCs [8].
- Short-term future work will be dedicated towards a fidelity improvement of the 1D analytical model by extending its capabilities towards sonic point and shock imposition. Hence, a wider range of operating conditions will be subject to investigation, allowing the previously mentioned quasi-stationary approach.
- In the longer term, a detailed geometry study and optimization using the presented 1D model, the design of a fully unsteady inlet boundary condition for the 3D LES, and optionally the fully integrated simulation of RDC and co-flow mixer (incorporating results from a parallel research activity) will be realized.

References

- International Civil Aviation Organization. ICAO Global Environmental Trends – Present and Future Aircraft Noise and Emissions. Report No. A40-WP/54, July 2019.
- International Energy Agency. World Energy Outlook 2021, December 2021.
- M. Asli, P. Stathopoulos, and C. O. Paschereit. "Aerodynamic investigation of guide vane configurations downstream a rotating detonation combustor". *Journal of Engineering for Gas Turbines and Power*, 143(6):061011, 2021. doi:10.1115/1.4049188.
- A. Naples, J. Hoke, R. Battelle, and F. Schauer. "T63 turbine response to rotating detonation combustor exhaust flow". *J. Eng. Gas Turbines Power*, 141(2), October 2018. ISSN 0742-4795. doi:10.1115/1.4041135.
- E. Tang. « Eléments de dimensionnement d'un éjecteur pour l'intégration d'une chambre à détonation rotative dans une turbine à gaz ». Technical report, Safran Tech, E&P, 2019.
- A. H. Shapiro. "The Dynamics and Thermodynamics of Compressible Fluid Flows", volume 1. John Wiley & Sons, 1953. ISBN 978-0471066910.
- T. Schoenfeld and M. Rudgeard. "Steady and unsteady flow simulations using the hybrid flow solver AVBP". *AIAA Journal*, 37(11), pp. 1378–1385, 1999, doi: 10.2514/2.636
- E. Bach, M. D. Bohon, C. O. Paschereit, and P. Stathopoulos. "Impact of outlet restriction on RDC performance and stagnation pressure rise". *AIAA Scitech 2019 Forum, AIAA 2019-0476*. 2019. doi: 10.2514/6.2019-0476.